

NON-NEWTONIAN CFD MODELLING OF A VALVE FOR MUD PUMPS

F. CONCLI¹ & C. GORLA²

¹Free University of Bolzano/Bozen, Faculty of Science and Technology, Bolzano, Italy.

²Politecnico di Milano, Department of Mechanical Engineering, Milano, Italy.

ABSTRACT

Mud pumps, like those used in the field of oil well drilling, are typically of the reciprocating type and are designed to circulate drilling fluid under high pressure down the drill string and back up the annulus. Automatic valves must be applied to the fluid end in order to grant the desired pumping effect. From the engineering point of view, the design of the valve geometry must ensure that the phenomenon of cavitation does not occur and that, during the pumping action, the stiffness of the reaction coil spring is able to avoid reaching the condition of end stroke of the valve.

Cavitation consists in the development of vapour cavities in the liquid phase. Inside the cavities, the pressure is relatively low. When subjected to higher pressure, the voids implode and generate an intense shock waves that promote the wear for the components (i.e. valve, valve seat, etc.).

A deep understanding of the fluid behaviour is crucial for an effective design.

Transient CFD simulations of the valve opening have been performed using a non-Newtonian fluid model able to describe the drilling muds. After a deep literature review, the Herschel-Bulkley model was selected as the most suitable for emulating the drilling mud.

With the abovementioned approach, the reaction spring and design the valve seat to avoid premature wear phenomena were properly designed.

The simulations have been also done considering a Newtonian fluid behaviour, in order to better understand the importance of considering the non-Newton behaviour for an effective design.

Keywords: cavitation, CFD, concrete, drilling mud, Herschel-Bulkley, pump, valve.

1 INTRODUCTION

The fluid flow inside a pump involves complex phenomena such as turbulence, unsteadiness and cavitation and for this reason, in the past, the design of the valves for the application to mud pumps has been mainly based on experimental tests and on the field experience. However, this approach can be very expensive and time-consuming.

In order to improve the design process of a pump, the capability of prediction the performances before manufacturing prototypes is crucial, but this is not trivial and implies complex calculation aimed at describing the behaviour of the flow of the pumped fluid. In the recent years, the developments in the fields of the Computer Science and of the Computational Fluid Dynamic (CFD) have made available reliable and effective tools for the simulation of the fluid flows, which can be applied in the design process.

The first attempts to apply CFD to the design of pumps were made about 30 years ago [1], and the first models were based on simplified Quasi-3D Euler conditions and potential flow solutions. Later, Reynolds Averaged Navier–Stokes (RANS) equations were introduced and eventually multiphase fluids and mass exchange models between the phases have been developed and included in many simulation codes.

Today, several CFD software, both commercial and open-source, are available and among those based on the traditional Finite Volume (FV) approach, the most widespread are Ansys Fluent [2] and OpenFOAM[®] [3].

These software include not only models for Newtonian but also for non-Newtonian fluids, as required for the simulation of particular fluids like muds and concretes.

The latest developments in fluid dynamics involve Lagrangian methods and Smoothed Particle Hydrodynamics (SPH) [4]. Dualsphysics [5] and nanoFluidX [6], just to mention some of them, are examples of such kind of simulation tools.

2 PROBLEM DESCRIPTION

Reciprocating pistons pumps are typically used for the circulation of muds circulate under high pressure during drilling operations or to pump fresh concrete.

The typical configuration of this kind of pump uses a triple piston/plunger. Each pump consists of three main sub-assemblies, the mechanical power transmission, the power end and the fluid end, as shown in Fig. 1.

In order to complete the pumping process the fluid end must be equipped with automatic valves, both for the suction – and for the pump delivery – port. Both valves are equipped with springs and when the piston is at the dead centres, the valves are closed. In particular, the valve on the suction port, which is the object of the investigation described in the present paper, prevents the backward flow of the fluid during the delivery phase, in which the fluid must flow through the delivery valve. The geometry of the valve and its opening height as a function of the delivered instantaneous flow must be carefully designed in order to avoid, or at least to minimize, cavitation effects which are the main responsible of the high-wear which can occur during operation. Also, the stiffness of the retaining spring must be defined properly, in order to avoid reaching the end of the valve stroke.

The inlet valve of the fluid end is opened during the suction phase, in which the motion of the piston (from the top dead centre to the bottom dead centre) produces a depressurization of the internal chamber. The pressure gradient between the internal and external surfaces of the inlet valve produces an hydraulic force, whose magnitude overcomes the reaction force of the (pre-loaded) spring, leading to the opening of the valve (the equilibrium position depends on the spring stiffness and the hydraulic force that is related to the motor speed and the fluid properties). In the phase described, the fluid is sucked in the pump chamber. At the end of the suction, the piston is in the bottom dead centre and inverts its motion starting to pressurise the chamber. The spring of the delivery valve is pre-loaded but is mounted outside the pressurized chamber (Fig. 2). The increasing pressure produces the opening of that valve and the pumping of the fluid.

The criticality related to cavitation phenomena occurs during the suction phase. During the pumping phase, in fact, the fluid is under high pressure. On the contrary, during the suction stage, the pressure is much lower and can locally sink down to the vaporization value), thus

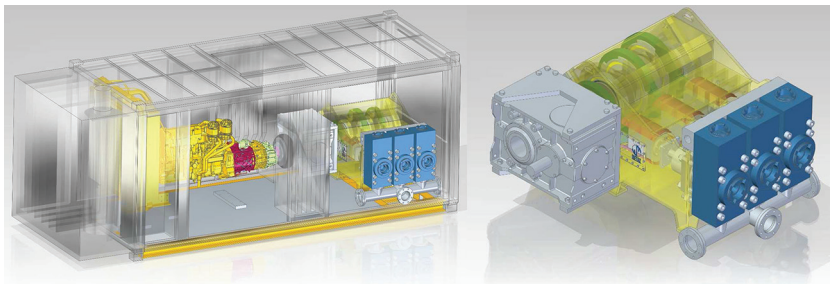


Figure 1: Typical example of a motor pump: mechanical power transmission (left), power end (centre) and fluid end (right).

Source: <http://www.jasonoandg.com/product/600s-triplex-plunger-pump.htm>

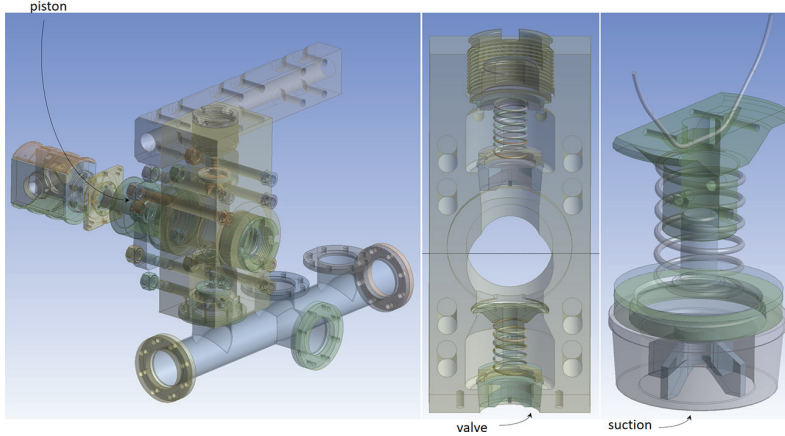


Figure 2: Typical layout of a fluid end of a triplex mud pump (left); fluid end (centre); suction valve (centre-right).

leading to a phase transition, from liquid to vapour, that is to cavitation. This phenomenon should be carefully avoided, in order to prevent excessive wear of the components: cavitation consists in the development of vapour cavities in the liquid phase which, when subjected to higher pressure, implode and generate intense shock waves that promote the wear of the components.

In order to avoid cavitation, a study of the fluid flow through the fluid-end and the valve was performed. The aim was to determine the pressure distribution, that can be then compared with the pressure of vaporization – that is a property of the fluid – in order to check if there are positions in which this value is reached or not. Knowledge of the minimum value of the pressure provide useful information for the definition of the performance of the booster pump, which is typically used to increase the pressure at the suction port, in order to avoid the cavitation.

The study of the pressure field is also useful to calculate the resultant load acting on the valve, which provides the basis to assess the stiffness of the retaining spring.

For this reasons, CFD simulations have been performed in order to verify the absence of cavitation during the operation, so to ensure an adequate life to the valves, and to calculate the loads that must be resisted by the retaining spring, without reaching the end stroke of the valve.

In the CFD simulation the properties of the fluid have been described taking into account of the non-Newtonian behaviour of the involved fluids.

3 MODELIZATION

The CFD simulations of the flow through an automatic suction valve have performed with Ansys Fluent: the extension of the domain modelled includes the liner, the piston, part of the pressurized chamber and the related components, like seals, spring, seat, etc.

In order to avoid mesh deformation and the related computational efforts and problems [8–10], simulations were performed keeping fixed the position of the valve (a).

In first step of the research steady state simulations were performed, with several constant values of the piston speed (and corresponding constant values of the flow) for each constant value of the valve position a . Taking into account the stiffness and the preload of the spring, it is possible to calculate, for each of the opening positions considered, the corresponding speed at the equilibrium and in this way the function of the valve position versus speed can be obtained.

In the second step of the research, in order to reduce the simulation time, a semi-transient approach was used, in which for each opening position a , the piston velocity was a function of the simulation time (to reproduce its simple harmonic motion induced by the crankshaft).

It has been verified that the two approaches produce the same practical results.

Just half of the domain was modelled taking advantage of the symmetry, so to reduce the amount of computational cells and speed up the numerical solution phase. All the boundaries were set to ‘walls’ except for the suction-section (inlet), the piston (outlet) and the symmetry plane. Table 1 reports the boundary conditions for p , v .

The model adopted for the CFD simulation solves two equations that mathematically represent the mass and momentum conservation equations, which can be written as:

$$\frac{\partial \rho}{\partial t} + \nabla \cdot (\rho \mathbf{u}) = 0 \quad (1)$$

$$\frac{\partial (\rho \mathbf{u})}{\partial t} + \nabla \cdot (\rho \mathbf{u} \mathbf{u}) = -\nabla p + \nabla \cdot [\boldsymbol{\tau}] + \rho \mathbf{g} + \mathbf{F} \quad (2)$$

ρ is the density, \mathbf{u} is the velocity vector, p is the pressure, \mathbf{g} is the gravitational force and \mathbf{F} a generic external force.

If the fluid is Newtonian, incompressible and the viscosity is constant, \boldsymbol{A} (shear stress) can be written as $\boldsymbol{A} = \mu (\nabla \mathbf{u} + \nabla \mathbf{u}^T)$. The relation between the shear stress and the shear rate is linear, passing through the origin, the constant of proportionality being the coefficient of viscosity μ .

Nevertheless, non-Newtonian fluids, like those typically processed by the pump under consideration, follow a different law of viscosity with respect to Newtonian ones. Most commonly, the viscosity of non-Newtonian fluids is a function of the shear rate. The fluid can even exhibit time-dependent viscosity. For this reason, a constant coefficient of viscosity cannot be defined.

As anticipated, fluids like concretes, muds and slurry [7] are non-Newtonian and have a behaviour that can be described by means of the Herschel–Bulkley model [11–13], which combines the features of both the Bingham Plastic and Power Law models and is already implemented in Ansys Fluent.

The Herschel–Bulkley is a generalized model of a non-Newtonian fluid, based on a non-linear stress–strain relation. The constitutive equation of the Herschel–Bulkley model is commonly written as:

$$\boldsymbol{\tau} = \tau_0 + \eta \mathbf{D} \quad (3)$$

in which \mathbf{D} is the rate-of-deformation tensor.

For low strain-rates $\dot{\gamma} < \dot{\gamma}_c = \tau_0 / \mu_0$ the ‘rigid’ material acts like a very viscous fluid with a viscosity μ_0 . As the strain rate increases and the yield stress threshold, τ_0 , is passed, the fluid behaviour is described by a power law.

Table 1: Boundary conditions.

Patch name	Symmetry	Suction	Piston	Valve	Housing
Type	Symmetry	Patch	Patch	Wall	Wall
p	$\nabla p = 0$	$p = \text{const}$	$\nabla p = 0$	$\nabla p = 0$	$\nabla p = 0$
\mathbf{u}	$\nabla \mathbf{u} = 0$	$\nabla \mathbf{u} = 0$	$\mathbf{u} = \text{const}$	$\mathbf{u} = 0$	$\mathbf{u} = 0$

For $\dot{\gamma} > \dot{\gamma}_c$

$$\eta = \frac{\tau_o}{\dot{\gamma}} + K \left(\frac{\dot{\gamma}}{\dot{\gamma}_c} \right)^{n-1} \tag{4}$$

For $\dot{\gamma} \leq \dot{\gamma}_c$

$$\eta = \frac{\tau_o}{\dot{\gamma}} \left(2 - \frac{\dot{\gamma}}{\dot{\gamma}_c} \right) + K \left((2-n) + (n-1) \frac{\dot{\gamma}}{\dot{\gamma}_c} \right) \tag{5}$$

in which $\tau = \eta(\mathbf{D})\mathbf{D}$ is the shear stress, $\dot{\gamma}$ is the shear rate, τ_o is the yield stress (that would allow cuttings to float under static conditions), k the consistency index and n the flow index. It is noted here that the concept of yield stress has been challenged [14] because a fluid may deform minutely at stress values lower than the yield stress. Nevertheless, yield stress may be considered to be an engineering reality and plays an important role. Estimated values of yield stress should be used only when experimentally-determined values are not available [15].

The fluid considered in the simulation is a fresh concrete, the parameters of which have been taken from literature [16–17] and are reported in Table 2. Nguyen reports the rheological characteristics for different water-concrete mixtures. Abrahamsson does not specify the exact composition of the mixture but, as Fig. 3 shows, the behaviour is compatible with a fresh concrete which Water-Concrete (W/C) ratio is between 0.5 and 0.55.

Table 2: Fluid parameters.

Model	τ_o [Pa]	k [Pa]	n [-]	ρ [kg/m ³]	$\dot{\gamma}$ [1/s]
Abrahamsson	8	2.5	0.35	1400	1
Nguyen W/C=0.5	8.1	3.87	0.408	1816	1
Nguyen W/C=0.55	5.6	1.84	0.454	1766	1

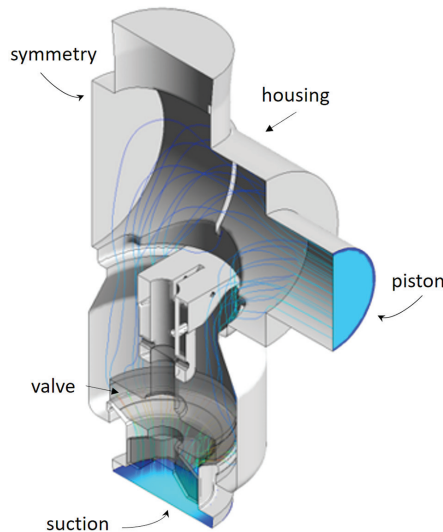


Figure 3: Domain and boundaries.

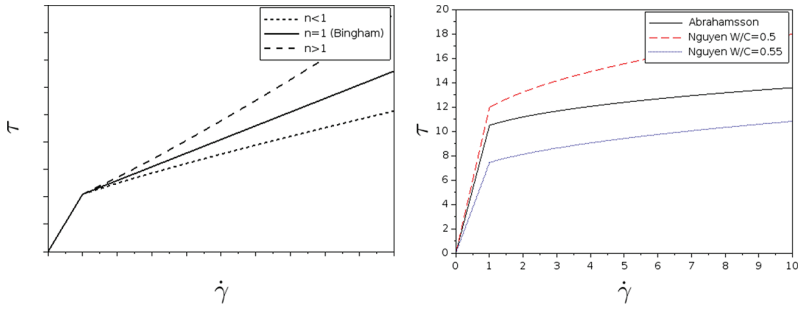


Figure 4: Variation of shear stress with shear rate according to the Herschel–Bulkley Model (left); Herschel–Bulkley Model according to Table 2.

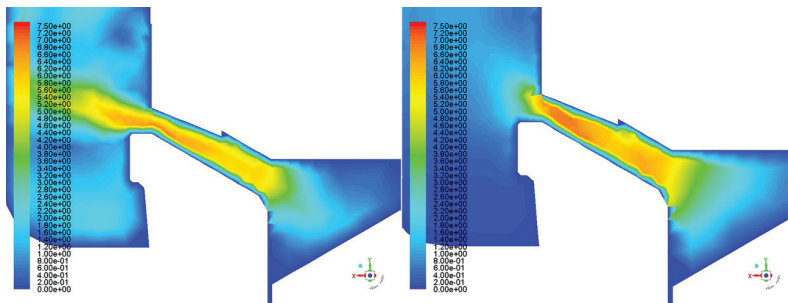


Figure 5: Velocity contours in the valve opening: non-Newtonian (left); Newtonian (right).

In order to appreciate the importance of modelling the non-Newtonian behaviour of the fluid (Fig. 4), in a first step of the research, the authors have also performed a comparison between the two types of fluids [18]: Figure 5 shows clearly the difference in terms of velocity profiles between a non-Newtonian (fresh concrete) and a Newtonian (water) fluid, for the same velocity of the piston and with the same valve position.

4 RESULTS OF THE SIMULATION

In addition to the results presented in [18], a different size of the valve has been simulated. In order to explore the behaviour of the valve in all the operating conditions, different valve openings ($a = 2 \text{ mm}$, $a = 5 \text{ mm}$, $a = 10 \text{ mm}$) have been simulated with variable piston positions (x) and velocities. The pictures reported in the following figures correspond to the time instant for which there is equilibrium between the force of the spring and the resultant of the pressure of the fluid.

Figure 6 also shows the resultant force on the valve for the different opening positions at the equilibrium.

The hydraulic force acting on the valve is a function of the valve opening (a) and the piston velocity. The maximum value at equilibrium (with the reaction of the spring) is in correspondence of the maximum valve opening considered ($a = 10 \text{ mm}$) for which there are the maximum speed and flow. In order to check for the cavitation, the minimum pressure takes place on the sharp edge of the valve (Fig. 6). Its magnitude is of about $-4\text{E}4 \text{ Pa}$ and this value, considering that the vaporization pressure of water is about $2.3\text{E}3 \text{ Pa}$, points out that cavitation could take place (Fig. 7). Nevertheless this effect can be avoided if the suction is fed by a booster pump, as usual for the application under consideration. With a usual value of the pressure of the booster pump pressure of 0 ($Dp > 1\text{E}5 \text{ Pa}$), the phenomenon can be prevented.

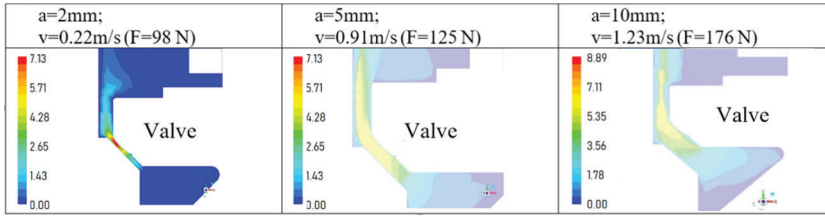


Figure 6: Velocity contours on the symmetry plane for different valve opening (a) at equilibrium positions (valve opening – piston velocity).

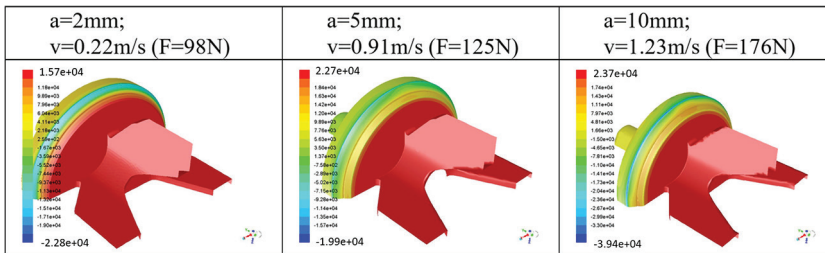


Figure 7: Pressure contours on the valve at equilibrium positions (valve opening – piston velocity).

Figure 8 shows the relation between the valve opening (a) and the piston speed (v): the relation is not linear. For low piston velocities (i.e. when the piston is near the top or bottom dead centre), the valve clearance (function of the valve opening a) is close to zero. Due to the viscous properties of the fluid, high local velocities take place in the gap between valve and valve seat. On the other side, when the valve position reaches its maximum, the clearance is much higher and the main contribution to the hydraulic forces is given by inertial effects.

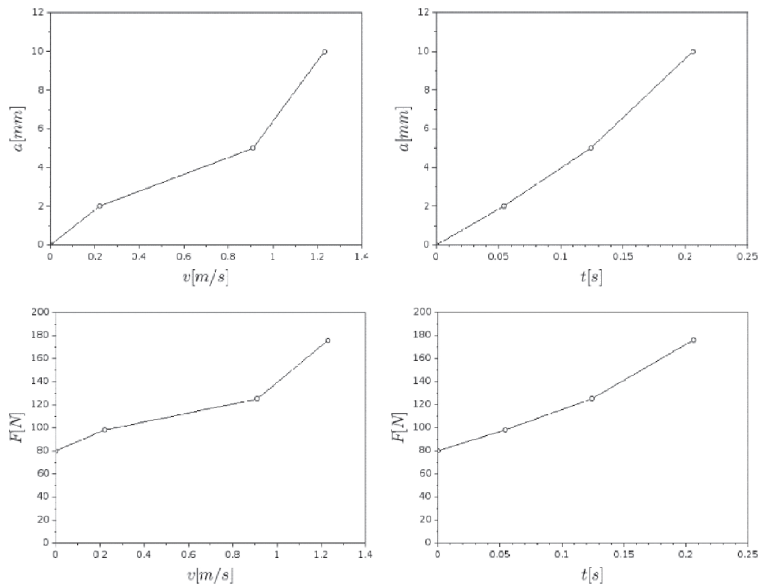


Figure 8: Valve opening (a) at equilibrium (top) and reaction force (F) of the spring (bottom) vs. piston speed (left) and time (right).

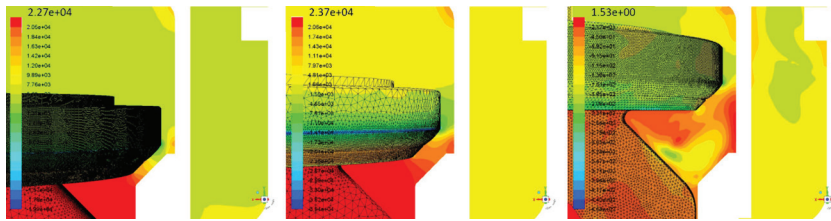


Figure 9: Pressure contours at different equilibrium positions (a).

5 PERFORMANCE ENHANCEMENTS

All the simulations have been performed on a Intel Xeon E5620@2,40 GHz x 2 (8 cores) 76.8 GFLOPS workstation with Ansys Fluent 17. In presence of small gaps [19], and specifically between the valve and the valve seat, the size of the mesh results significantly reduced and the computational time increases significantly. Some specific techniques can be applied when the viscous contribution can be neglected [20–21], but this is not the case. Despite the symmetry, more than 2 million cells are required in order to properly discretize the domain. This has led, on the above mentioned workstation, on a computational effort for each semi-transient simulation (with fixed valve position) of about 15 h per simulation.

6 CONCLUSIONS

CFD has been applied to simulate the flow of a non-Newtonian fluid through the automatic valve on the suction side of a fluid end of a reciprocating pump. CFD has proved to be able to provide tools simulations that can be effectively applied to improve the design and analysis of complex systems such as the type of pumps considered.

The simulation have been effectively applied to determine the equilibrium position of the valve, which depends from the pressure and velocity fields that are, in turn, function of the piston velocity and the fluid properties and therefore has provided the information necessary to check the stiffness and the preload of the retaining spring. This is an important step in the assessment of the design of the pump and traditionally it was based only on experience and experimental tests.

It has been verified that a semi-transient approach, in which the valve opening was kept fixed while the piston velocity was a function of the time, it is possible to find the equilibrium position of the valve without repeating several stationary simulations with many speed values for each valve opening.

Cavitation is a phenomenon that should be avoided in order to reduce the wear of automatic-valves: thanks to the CFD simulation it has been calculated the minimum pressure during the pumping operations and on the basis of this value it is possible to define the performance required to the booster pump.

REFERENCES

- [1] Shah, S.R., Jain, S.V., Patel, R.N. & Lakhera, V.J., CFD for centrifugal pumps: A review of the state-of-the-art. *Procedia Engineering*, **51**, pp. 715–720, 2013. <https://doi.org/10.1016/j.proeng.2013.01.102>
- [2] Ansys. www.ansys.com
- [3] OpenFOAM(R). www.openfoam.com
- [4] Concli, F. & Gorla, C., Windage, churning and pocketing power losses of gears: different modelling approaches for different goals [Wirkungsgrad und Verluste von Zahnradgetrieben: Verschiedene Methoden für verschiedene Anwendungen]. *Forschung*

- im Ingenieurwesen/Engineering Research*, **80(3–4)**, pp. 85–99, 2016. <https://doi.org/10.1007/s10010-016-0206-9>
- [5] DualSPHysics. <https://dual.sphysics.org>
- [6] NanoFluidX. <http://www.fluidyna.com/content/nanofluidx>
- [7] Bietresato, M., Friso, D. & Sartori, L., An operative approach for designing and optimising a pipeline network for slurry collection from dairy farms across a wide geographical area. *Biosystems Engineering*, **115(3)**, pp. 354–368, 2013. <https://doi.org/10.1016/j.biosystemseng.2013.01.008>
- [8] Concli, F. & Gorla, C., Numerical modelling of the churning power losses in planetary gearboxes: An innovative partitioning-based meshing methodology for the application of a computational effort reduction strategy to complex gearbox configurations. *Lubrication Science*, **29(7)**, pp. 455–474, 2017. <https://doi.org/10.1002/ls.1380>
- [9] Concli, F., Thermal and efficiency characterization of a low-backlash planetary gearbox: An integrated numerical-analytical prediction model and its experimental validation. *Proceedings of the Institution of Mechanical Engineers, Part J: Journal of Engineering Tribology*, **230(8)**, pp. 996–1005, 2016. <https://doi.org/10.1177/1350650115622363>
- [10] Concli, F., Gorla, C., Stahl, K., Höhn, B.-R., Michaelis, K., Schultheiß, H. & Stemplinger, J.-P., Load independent power losses of ordinary gears: Numerical and experimental analysis. *5th World Tribology Congress, WTC 2013*, **2**, pp. 1243–1246, 2013.
- [11] Herschel, W.H. & Bulkley, R., Konsistenzmessungen von Gummi-Benzollösungen. *Kolloid-Zeitschrift*, **39(4)**, pp. 291–300, 1926. <https://doi.org/10.1007/bf01432034>
- [12] Herzhaft, B., Rousseau, L., Neau, L., Moan, M. & Bossard, F., Influence of temperature and clays/emulsion microstructure on oil-based mud low shear rate rheology. *SPE Journal*, **8(3)**, pp. 211–217, 2003. <https://doi.org/10.2118/86197-pa>
- [13] Kenny, P. & Hemphill, T., Hole-cleaning capabilities of an ester-based drilling fluid system. *SPE Drilling & Completion*, **11(1)**, pp. 3–9, 1996. <https://doi.org/10.2118/28308-pa>
- [14] Walters, K., *An Introduction to Rheology*, Vol. 3, Elsevier Science, 1989.
- [15] Rao, M.A., *Rheology of Fluid, Semisolid, and Solid Foods, Food Engineering Series*, Springer Science+Business Media: New York, 2014.
- [16] Abrahamsson, J., Product losses of highly viscous products in pipe systems during displacement processes, Thesis for the Degree of Master of Science Division of Fluid Mechanics Department of Energy Sciences Faculty of Engineering Lund University, 2011.
- [17] Nguyen, V.H., Rémond, S., Gallias, J.L., Bigas, J.P. & Muller, P., Flow of Herschel–Bulkley fluids through the Marsh cone. *Journal of Non-Newtonian Fluid Mechanics*, **139(1–2)**, pp. 128–134, 2006. <https://doi.org/10.1016/j.jnnfm.2006.07.009>
- [18] Concli, F. & Gorla, C., Analysis of an automatic valve geometry for concrete and drilling mud pumps to avoid cavitation: Non-newtonian CFD modelling. *WIT Transactions on Engineering Sciences*, **120**, pp. 209–217, 2018. doi: 10.2495/AFM180211
- [19] Concli, F. & Gorla, C., Analysis of the oil squeezing power losses of a spur gear pair by mean of CFD simulations. ASME 2012 11th Biennial Conference on Engineering Systems Design and Analysis, ESDA 2012, 2, pp. 177–184, 2012.
- [20] Concli, F. & Gorla, C., Oil squeezing power losses in gears: A CFD analysis. *WIT Transactions on Engineering Sciences*, **74**, pp. 37–48, 2012.
- [21] Concli, F., Della Torre, A., Gorla, C. & Montenegro, G., *A New Integrated Approach for the Prediction of the Load Independent Power Losses of Gears: Development of a Mesh-Handling Algorithm to Reduce the CFD Simulation Time*. *Advances in Tribology*, 2016, art. no. 2957151, 2016.